

# Martian Microprobe Entry, Descent, and Landing System

Stanley Krzeński<sup>1</sup>, Periklis Papadopoulos<sup>2</sup>

<sup>1</sup>Masters Student, Department of Aerospace Engineering, San Jose State University

<sup>2</sup>Professor, Department of Aerospace Engineering, San Jose State University



## Introduction

Significant advances in system miniaturization in the last couple decades have allowed for the potential of interplanetary probes to be built in the ubiquitous CubeSat form factor (CFF), as well as the smaller PocketQube form factor. Deep-space probes in the CFF have most recently been demonstrated by MarCO, and will soon be expanded by the thirteen CubeSats scheduled for launch on Artemis I. However, to date, the Deep Space 2 probes represent the only CFF-size ("microprobe") landers sent to Mars - no data was returned as they were lost [1]. In order to allow mature, microelectromechanical systems (MEMS)-enabled probes to enable new methods of in-situ exploration, such as through the Internet of Things (IoT) paradigm, a combination of heritage systems, COTS products, and system-on-circuit-board methods may be employed. The system is designed from a top-down systems engineering approach, starting with launch vehicle compatibility, followed by thermal protection sizing to determine an appropriate mass fraction. An application is presented, which is part of current research at San Jose State University to leverage this concept.

## Launch Vehicle and EDLS Sizing

This EDLS is intended to be a secondary payload to another Martian interplanetary mission. The primary requirement is to fit within an ESPA 6-15-24 port, reducing the volume requirements in a fairing, illustrated in Figure 1. This would allow two opportunities: the ability to launch and deploy multiple units as part of a secondary payload, or a dedicated mission with lightweighted, stacked ESPA rings to distribute a networked system throughout Mars.

Keeping the ballistic coefficient within family was also a primary concern; this drove total deliverable mass and reduced aerothermal analysis requirements. Table 1 [2] shows the range of this family of landers.

For a frontal area of 0.09 m<sup>2</sup> and a C<sub>d</sub> of 1.827, the maximum system mass attainable is 12.5 kg by taking the median BC between MPF and MSL, which was 76.0 kg/m<sup>2</sup>. The C<sub>d</sub> was obtained through a finite rate nonequilibrium CFD solution during peak heating velocity. Due to retro-propulsion limitations, this was later revised down to 6.5 kg, or 39.5 kg/m<sup>2</sup> ballistic coefficient.

## Thermal Protection

Due to the large heritage of Martian EDLS available, minimal analysis was needed. Lockheed Martin's SLA-561V ablator was selected for this micro EDLS due to said heritage [4]. The density was assumed to be 0.51 g/cc based on AVCOAT 5026-39 [5]. Szalai et. al. (2011) presented the analysis of remains of the MER Opportunity heatshield from 2004, and concluded that only 4.8 of 15 mm had recessed from the "flank" during entry [6]. Implemented as-is, not including bonding to the structure, this would yield 0.7 kg ablator, or 10.7% of total vehicle mass. Including 15 mm of ablator will also permit a larger launch window.

To verify the heat flux during the peak heating condition fell within the range shown in Table 1, as well as other aerodynamic parameters, ANSYS Fluent was used for hypersonic, finite-rate chemistry. Because Mars-GRAM 2010 yielded a P<sub>inf</sub> of 1.73 Pa at 50 km MOLA, P<sub>inf</sub> was increased to 200 Pa to ensure continuum flow.

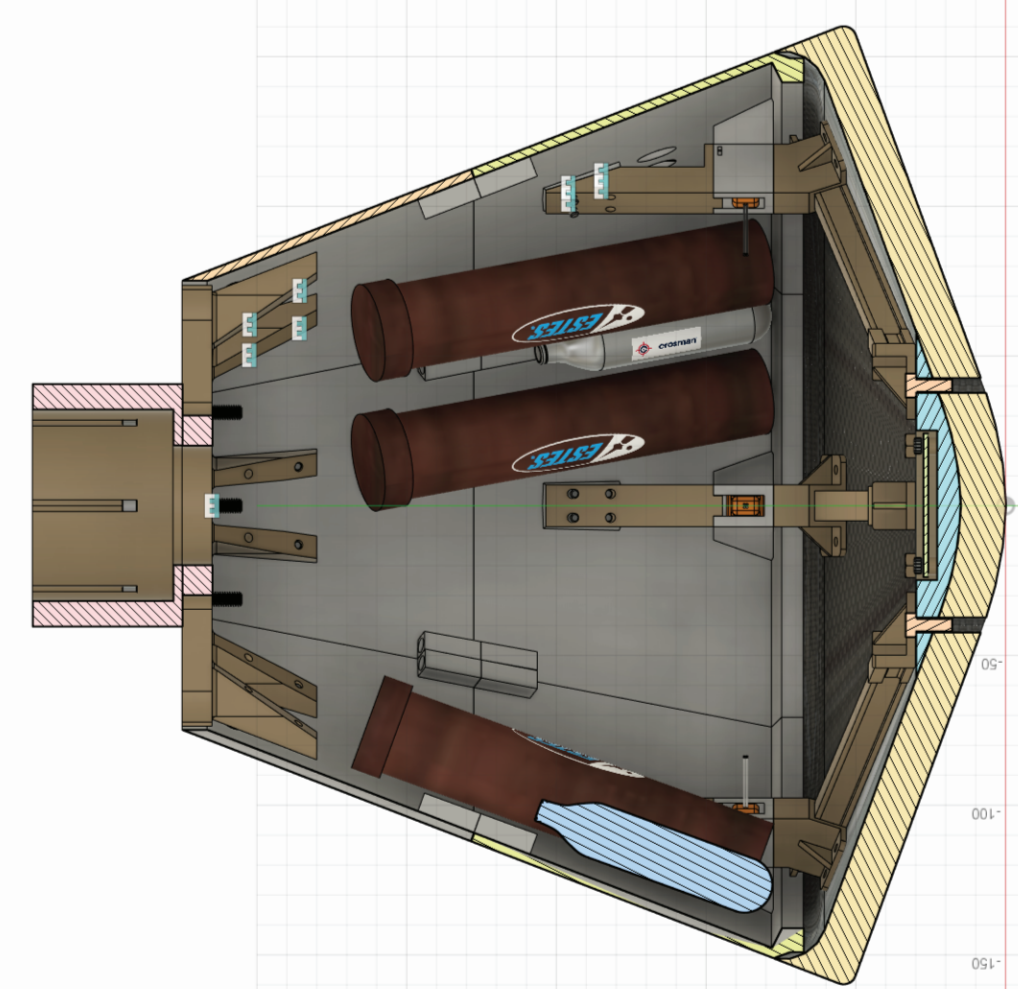


Figure 2: Forebody heat flux profile.

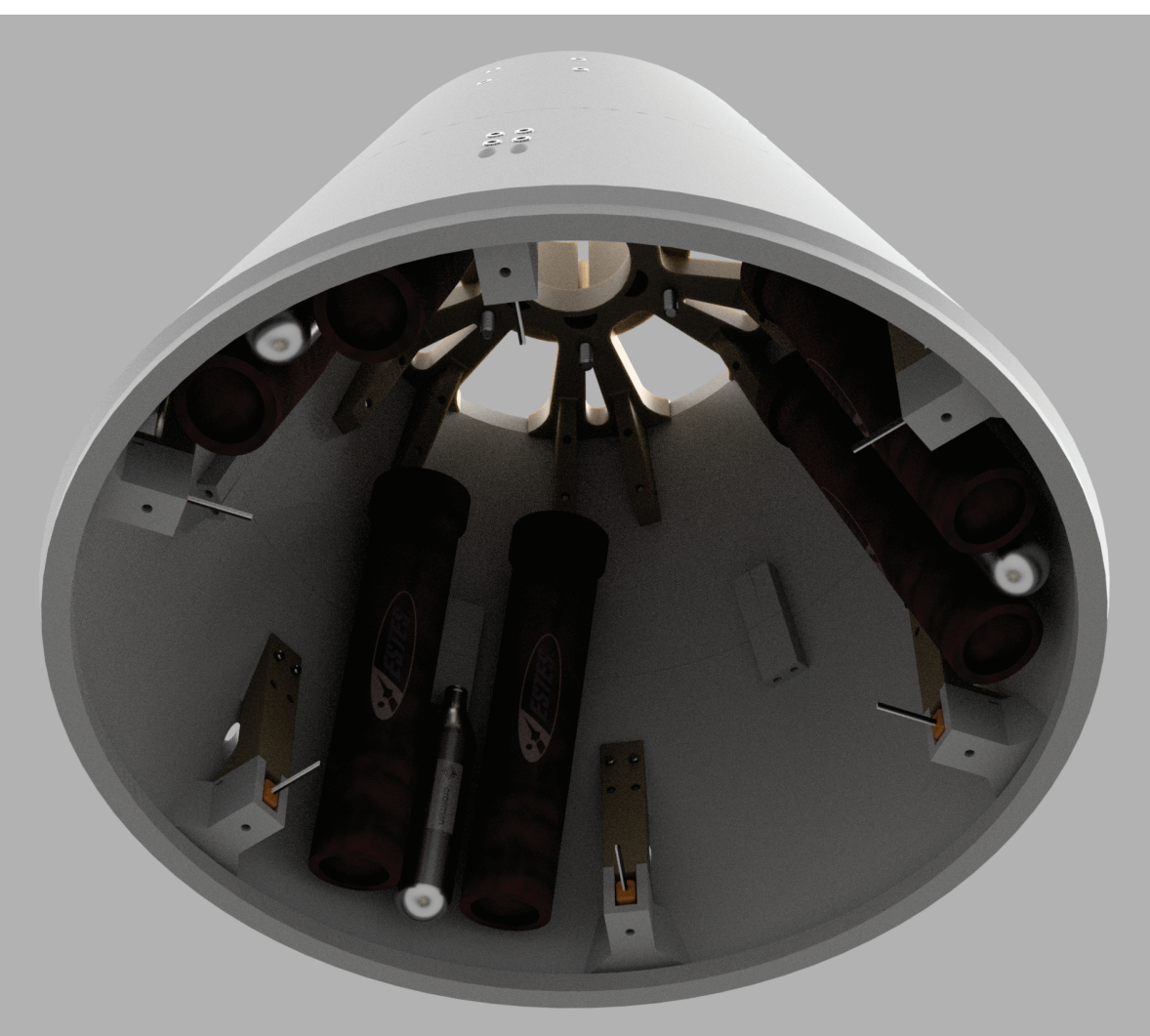


Figure 3: Backshell CAD interior detail.

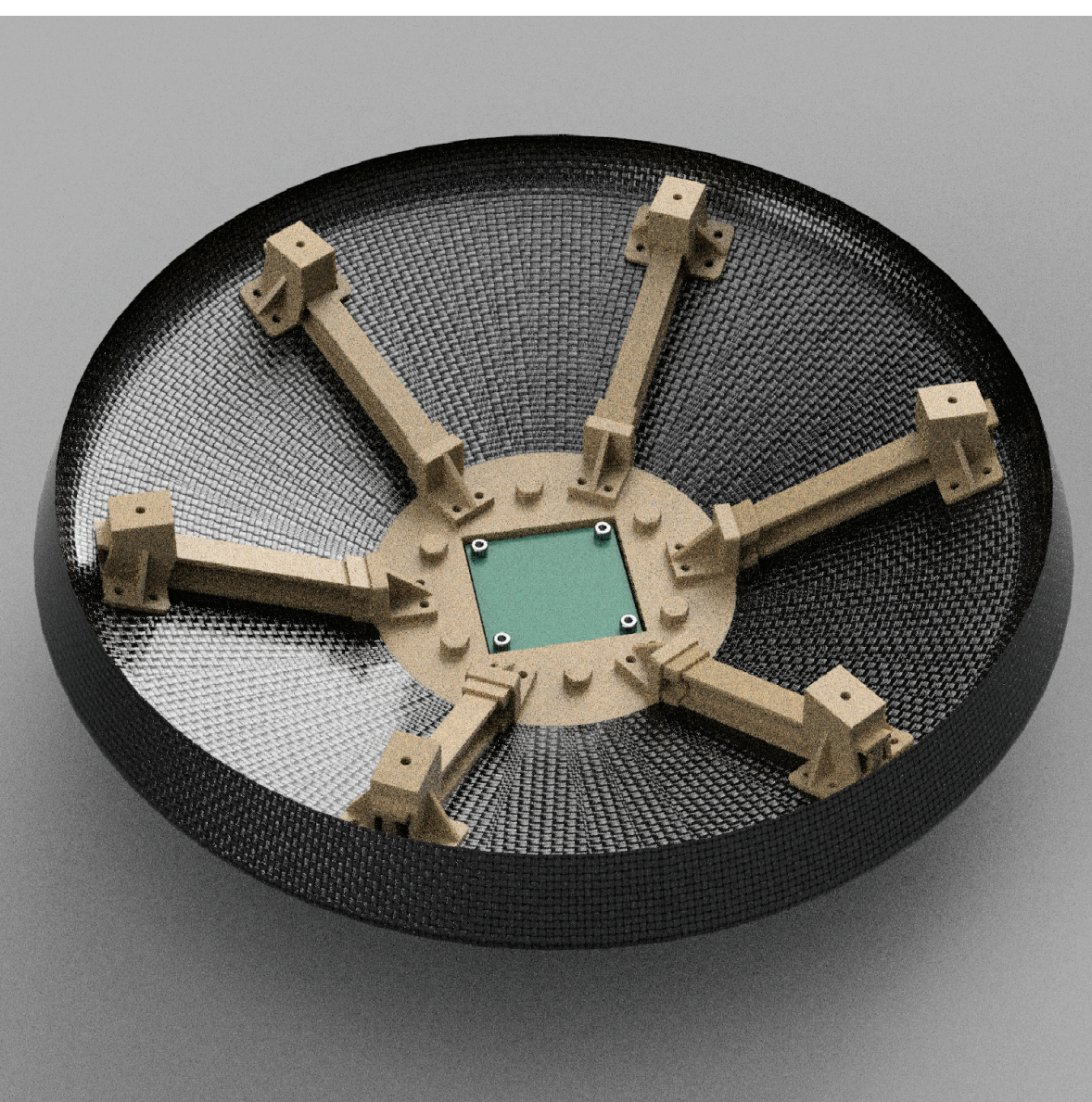


Figure 4: TPS with PAEK ribs. Aerodynamics package at center.

Table 1: Key parameters from Mars EDL systems.

Vehicle	V <sub>0</sub> (km/s)	Ballistic Coefficient	Heat Flux (W/cm <sup>2</sup> )
Viking	4.5	63.7	24
MPF	7.5	62.3	118
MER	5.5	89.8	50
MSL	5.6	110	95

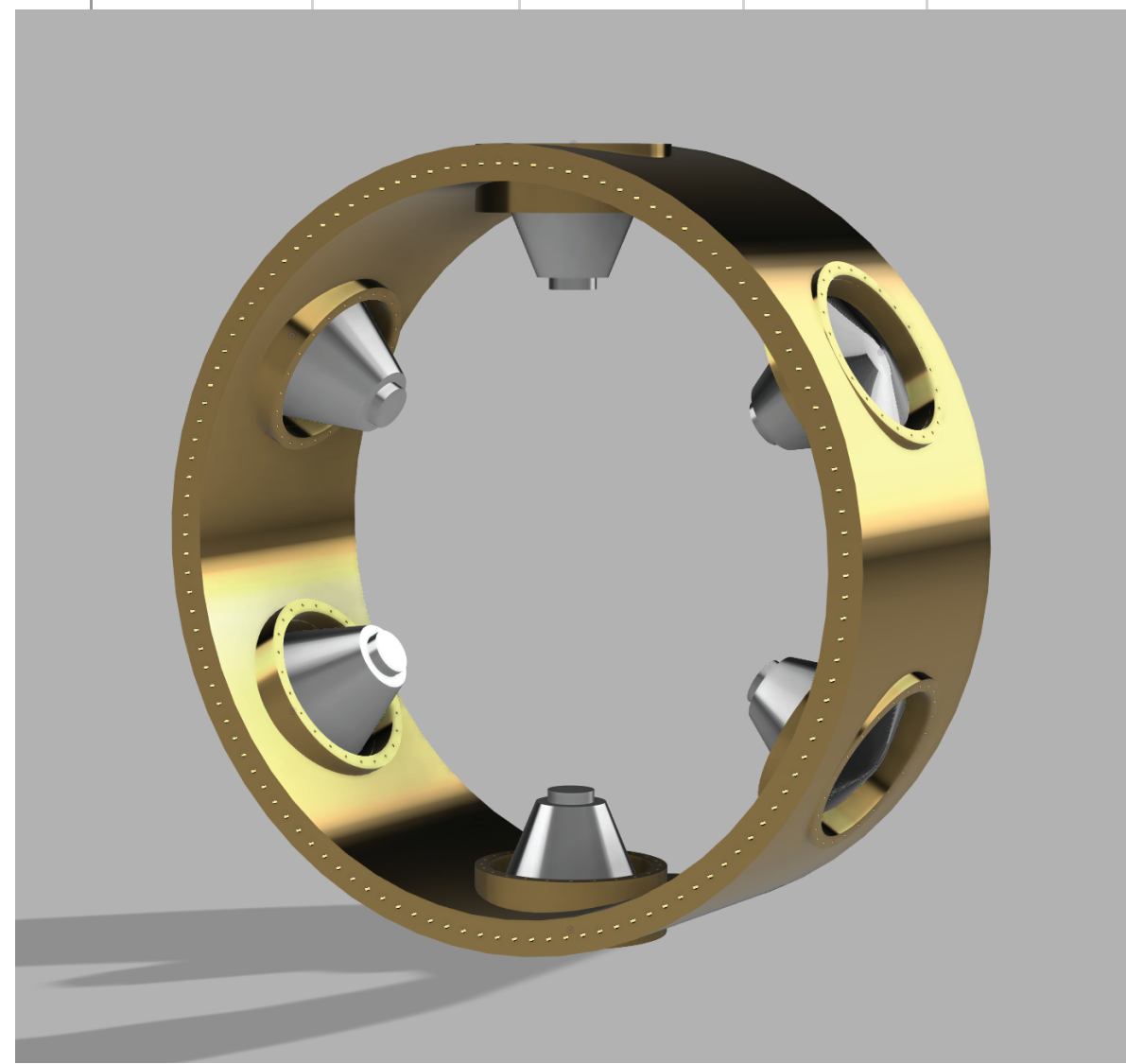


Figure 1: ESPA ring with six microprobes.

## Structure

Thermoplastics and photopolymer resins used in additive manufacturing (AM) may enable the structure of this EDLS, including backshell and forebody structure, to be almost entirely constructed using composite AM, aside from the TPS material. In particular, certain brands of carbon fiber reinforced polyaryletherketone (PAEK) would be suitable candidates [7], due to heritage usage in LEO and on the Juno mission [8]. Testing of PAEK-based composite materials by Martin Marietta in the 90's [9] supports the claims in [7] and [8] for wide temperature usage. Current commercial AM systems are capable of repeatable, "large-format" prints with PAEK.

Assembly of the structure would use low-offgassing epoxies in combination with lock nut and bolt fasteners, rated for low temperatures. Verification of mechanical launch and EDL load survival would be through both modal analysis and vibration table testing. Figure 2, 3 and 4 show the main components of the spacecraft, which also highlights the ribbed structure.

The SMAD, third edition, reports that starting points for spacecraft structural mass is 10-20% [10]. Due to anticipated loads in excess of 20g during touchdown [11], a 20% mass is assumed.

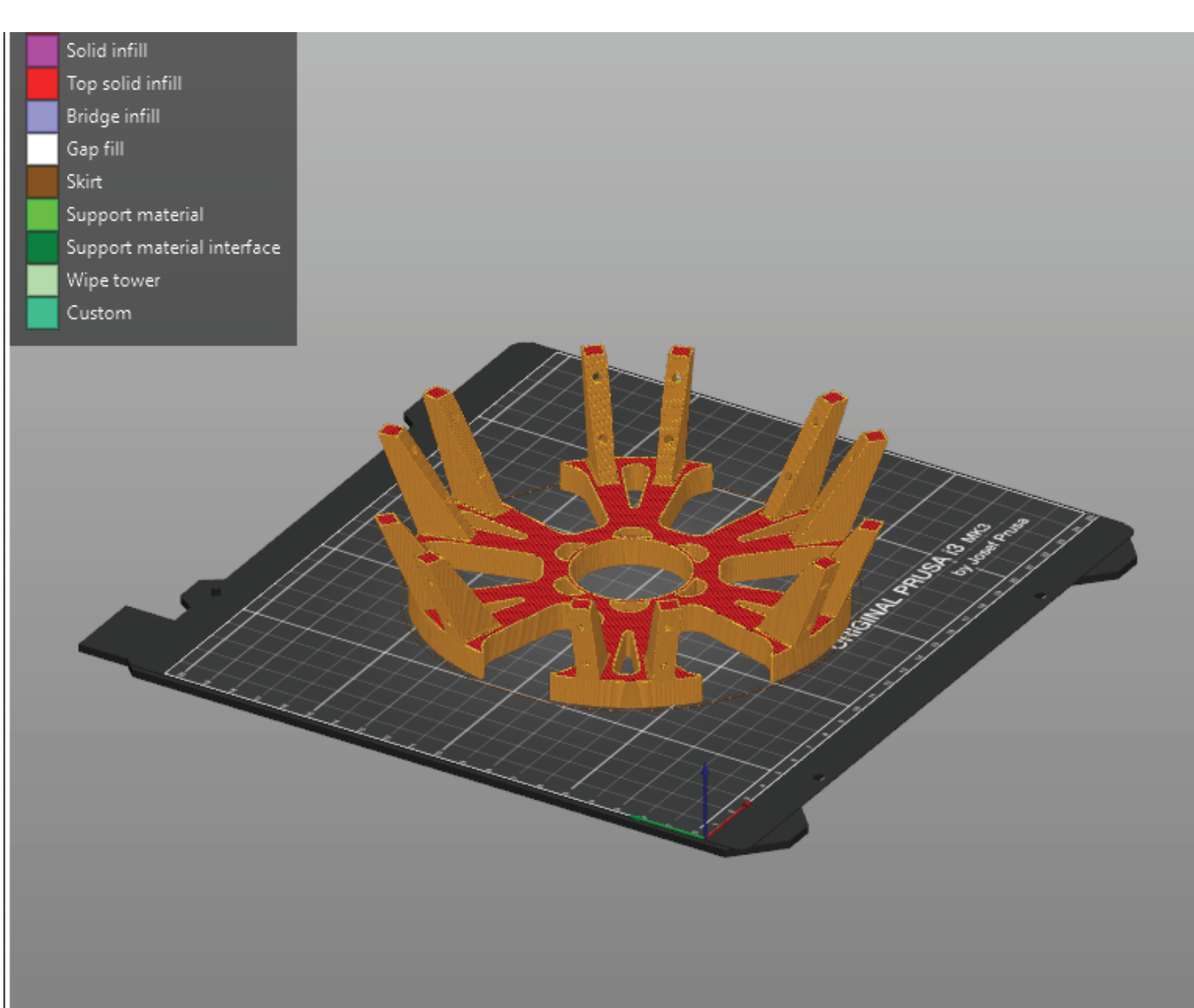


Figure 5: Additive manufacturing of structural components.

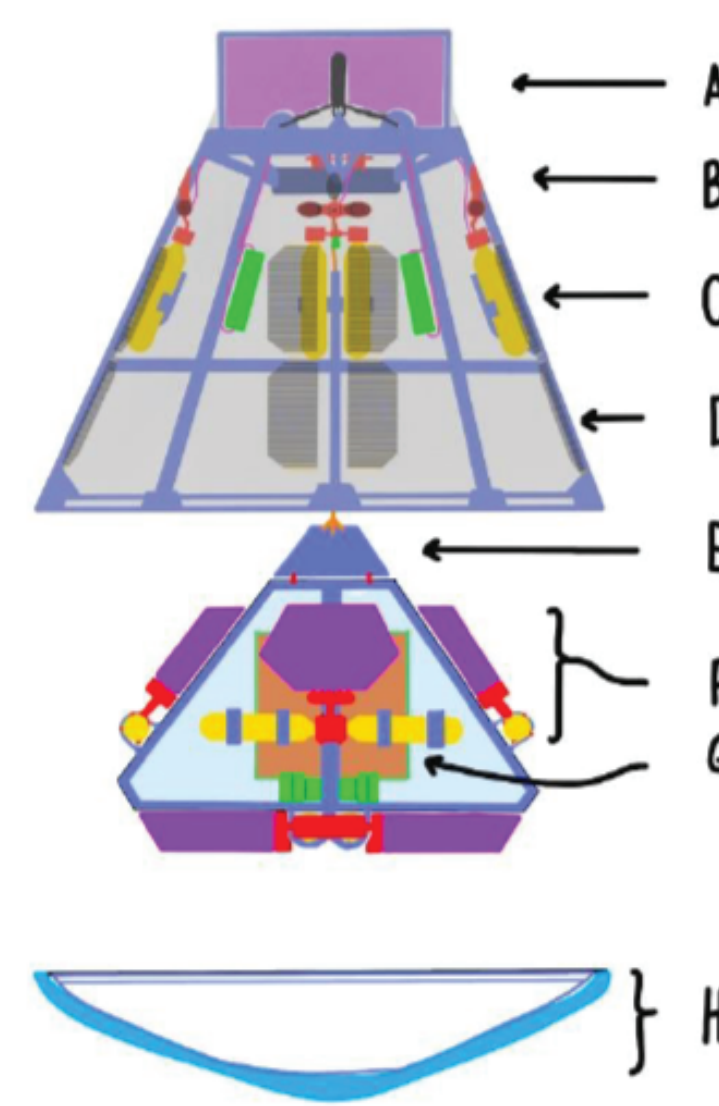


Figure 6: Main components of EDLS with representative payload (orange cube). A: DGB parachute. B: Cold-gas thruster clusters. C: COTS CO<sub>2</sub> cartridges. D: Solar cells (black), ribbed PAEK-CF structure (blue). E: Bridle to tetrahedron clamp. F: Airbag units. Purple: airbags; red: valve and coupling mechanisms; yellow: CO<sub>2</sub> cartridges. G: 1U nominal payload volume. H: SLA-561V/PAEK-CF heat shield. The system has a very similar look to MPF and MER, but is extruded, similar to Gemini and Mercury, in order to fit more entry systems.

## Concept of Operations

As a secondary spacecraft assumed to be released from an ESPA carrier near entry, the micro EDLS will briefly be a free-flyer. Ephemeris would be loaded to each EDLS from the primary spacecraft before release. This would enable final, fine course adjustments, as well as the possibility to fly a trajectory on entry. Attitude control is provided by cold gas thrusters powered by COTS CO<sub>2</sub> cartridges, as well as a mass-shifting mechanism leveraging the less stable, "tall" configuration. Assuming a 60s specific impulse and 1 g/sec consumption, 600mN would be generated, with 30 mN minimum impulse for 50 mS pulses. This would be sufficient for spinup as a free flyer and limited targeting during entry.

Table 2: Mass summary of microprobe EDLS. The remaining mass available for payload is similar to MSL - 23.4% of MSL comprised of Curiosity,

Microprobe EDLS Mass Budget		
Component	Percent Mass (%)	Mass (kg)
SLA-561V TPS	10.7	0.7
3x "12g" CO <sub>2</sub> cartridges - Airbag	1.97	0.128
3x "12g" CO <sub>2</sub> cartridges - RCS	1.97	0.128
6x Estes F15-0 retro motors	8.8	0.57
PAEK petal tetrahedral structure	6.15	0.4
PAEK monocoque structure and ribs	6.15	0.4
316L stainless fasteners	3.07	0.2
Batteries, electronics, TPS pyros	8	0.52
RCS - regulator and thrusters	5	0.33
20% margin	20	1.3
Remaining mass for lander payload	28.19	1.824

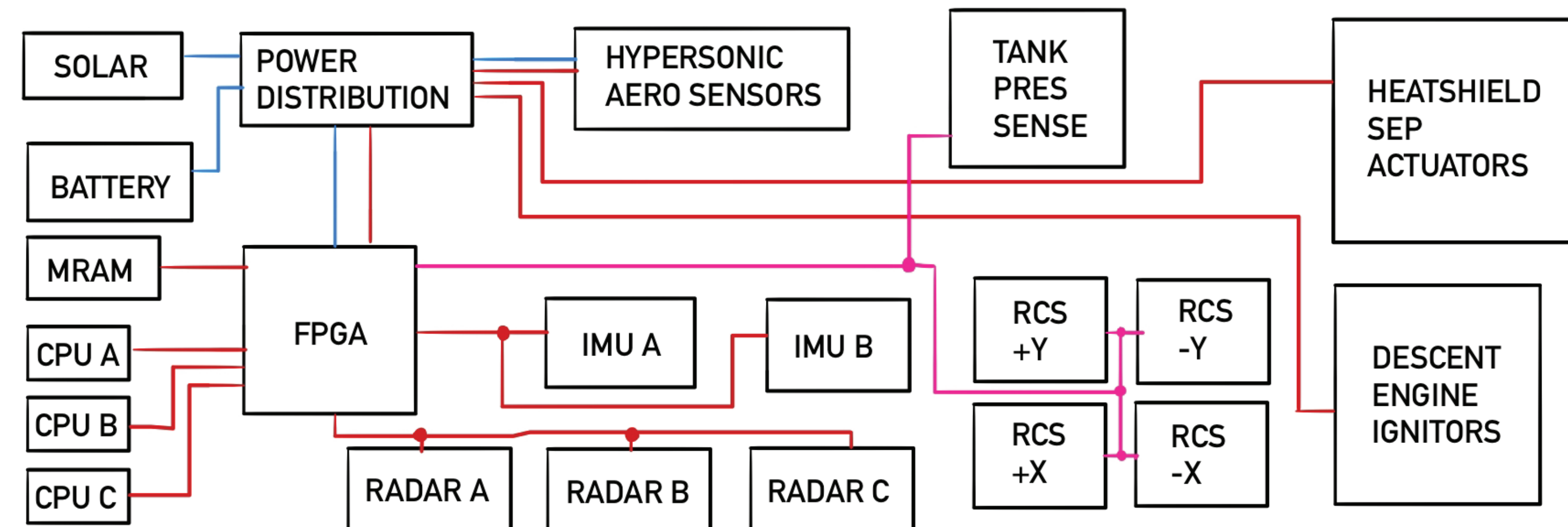


Figure 7: Top-level electronic system diagram. A rad-tolerant FPGA will be used to provide a system bus and lockstep redundancy management. Standard I<sup>2</sup>C, SPI, and 1553C will communicate between individual systems, with a 1553C link to the payload if necessary.

Similar to MPF and MER, we adapt the airbag-retrorocket mechanism developed by JPL to conduct the final landing portion due to heritage, and due to the ability to scale down. Hobby APCP motors would be used to slow the lander down just before landing. Initially, LIDAR was considered for a retrorocket firing solution, but would be too unreliable as a ground solution would likely be determined too late due to very weak returns. Infineon produces a compact, Ka-band radar designed for distant human detection [12]. This radar can easily be configured to operate in pulsed-Doppler mode. Multiple units would be installed in the backshell for redundancy.

Triple redundant, rad-hard 32-bit ARM-based CPUs with a rad-tolerant FPGA redundancy controller would form the main management computer, controlling all aspects of EDL. By centralizing control to one set of processors, the cost of the system can be lowered; though upfront software V&V costs will be higher.

## Applications and Future Work

Distributed sensing on Earth has many benefits in many fields; the same concept can be applied to interplanetary destinations such as Mars. Launching a dedicated mission composed of weather stations, nephelometers, spectrometers, and other environmental monitoring sensors in MEMS form would vastly improve the quality of remote sensing data by providing "ground truth" in dozens of locations. Rugged MEMS tiltmeters can be used as coarse seismometers to gain further insight into wide-scale geological conditions, or the origins of global dust storms could be determined in real-time with weather stations.

Further work is presently underway to constrain specifics of the design, such as further CFD analysis along the entire trajectory, including during final descent to determine bridle cut times and parachute sizing. Finite-element analysis will need to be performed to assess further reductions in mass, in addition to reduction of margin. Additionally, an IoT-based mission is being designed and developed to complement this EDLS. Reductions in mass and volume optimization may allow secondary payloads mounted outside of the 1U nominal volume.

## References

- [1] Siddiqi, A. (2018). *Beyond Earth*. NASA SP-2018-4041.
- [2] Lockwood, M. K., et. al. (2007). MSL EDL Performance and Environments. Conference Paper, 2nd IPPW. <https://ntrs.nasa.gov/citations/20070014674>
- [3] MOOG Defense & Space (2020). ESPA User Guide. [https://www.moog.com/content/dam/moog/literature/Space\\_Defense/spaceliterature/structures/moog-espas-users-guide-datasheet.pdf](https://www.moog.com/content/dam/moog/literature/Space_Defense/spaceliterature/structures/moog-espas-users-guide-datasheet.pdf)
- [4] Tran, Huy, et. al. (1996). Ames Research Center Shear Tests of SLA-561V Heat Shield Material for Mars Pathfinder. [https://ntrs.nasa.gov/archive/nasa/casi.ntrs.nasa.gov/19960049758\\_1996080506.pdf](https://ntrs.nasa.gov/archive/nasa/casi.ntrs.nasa.gov/19960049758_1996080506.pdf)
- [5] (1968). Flight Test Analysis of Apollo Heat-Shield Material Using the Pacemaker Vehicle System. NASA TN-D-4713. [https://ntrs.nasa.gov/archive/nasa/casi.ntrs.nasa.gov/19680021275\\_1968021275.pdf](https://ntrs.nasa.gov/archive/nasa/casi.ntrs.nasa.gov/19680021275_1968021275.pdf)
- [6] Szalai, C., et. al. (2011). Mars Exploration Rover Heatshield Observation Campaign. AIAA 11-2340. <https://hdl.handle.net/hdl:2014/42204>
- [7] 3DXTECH CF-PEEK-C. <https://www.3dxtech.com/product/carbonx-cf-peek-c-aerospace/>
- [8] Zortrax Z-PEEK. Zortrax SA, Poland. <https://zortrax.com/filaments/z-peek/>
- [9] Rawal, S., Misra, M. (1992). Measurement of Mechanical and Thermophysical Properties of Dimensionally Stable Materials for Space Applications. Martin Marietta Astronautics Group, Denver, CO. <https://ntrs.nasa.gov/api/citations/19920011035/downloads/19920011035.pdf>
- [10] Larson, W., Wertz, J. (1999). *Space Mission Analysis and Design*. p. 336. Microcosm Press: El Segundo, CA.
- [11] Spencer, D., et. al. (1998). Mars Pathfinder Entry, Descent, and Landing Reconstruction. *Journal of Spacecraft and Rockets*. <https://doi.org/10.2514/2.3478>
- [12] Infineon Sense2GoL Development kit. [https://www.infineon.com/dgdl/Infineon-Sense2GoL%20Pulse-ProductBrief-v01\\_00-EN.pdf?fileId=55464626eab8fb016eb7b647e40f3f](https://www.infineon.com/dgdl/Infineon-Sense2GoL%20Pulse-ProductBrief-v01_00-EN.pdf?fileId=55464626eab8fb016eb7b647e40f3f)